Imaging of micro- and nano-structures with hard X-rays

C. Rau, V. Crecea, C.-P. Richter, K.M. Peterson, P.R. Jemian, U. Neuhäusler, G. Schneider, X. Yu, P.V. Braun, T.-C. Chiang and I.K. Robinson

Abstract: Imaging of micro- and nano-structures of opaque samples is demonstrated using hard X-rays. Two different methods are employed with an instrument recently built at the beamline 34 ID-C at the Advanced Photon Source. In-line phase contrast micro-imaging has been performed with highly coherent radiation. For the characterisation of structures as small as 50 nm, a hard X-ray microscope has been built. These complementary techniques cover a large range of length-scales.

1 Introduction

For understanding the macroscopic properties of matter, often a detailed knowledge of its microstructure is necessary. Therefore experimental non-invasive tools with sub-micron resolution are essential. For example materials containing a regular refractive index modulated by a periodic sub-micrometer pattern can exhibit a photonic band gap (for a review about this subject see [1]). In the mammalian inner ear, tissue vibration amplitudes of a few nanometres result in the generation of electrical signals—the action potentials—which encode the acoustic information, leading to hearing sensation [2–4]. For both examples, it is important to study the structures with sub-micron resolution without destroying the integrity of the structure. However, contemporary methods often either lack sufficient spatial resolution and/or sensitivity (like NMR) or cannot image the structure of interest [5].

Methods providing high spatial resolution often require extensive sample modifications. However, sample modifications bias the experimental results or make the study impossible. For example soft tissue in the cochlea has been studied using light microscopy. Samples had to be fixed, dehydrated, and embedded before being sliced with a microtome. Furthermore, for dynamical measurements, the cochlea should not be altered and should be made in vivo without opening it.

Hard X-ray imaging is an excellent tool to examine structures on the micro- and nanometre length scale. For high photon energies, bulk materials become translucent because of the high penetration depth of the radiation. Furthermore, hard X-ray imaging is possible under various external thermal and mechanical conditions.

With the development of powerful light sources, novel hard X-ray imaging techniques have evolved. Third generation synchrotrons are optimised radiation sources for X-ray science, providing highly coherent and intense X-ray light at high photon energies, with a high penetration depth into the sample.

When imaging soft tissue or very small objects, the contrast due to the absorption of X-ray photons is very weak. However, the phase shift that occurs when a light wave propagates through material of different optical density can still be significant. Phase contrast imaging methods transform the phase shift information into amplitude, which is measurable with a detector. Structures with small absorption contrast or smaller than the detector resolution (in particular when using in-line phase contrast) can still be imaged. In-line phase contrast imaging is based on the propagation of X-rays in the near-field. The distance between detector and sample $d_{\text{det-sam}}$ is small, compared to the objects' smallest structures s_{obj} to resolve ($d_{\text{det-sam}} \ll s_{\text{obj}}^2/\lambda$, λ is the wavelength of the X-rays) and is typically in the order of several millimetres to centimetres for the given energies. The detected image closely resembles the sample structure with its edges enhanced. Phase contrast imaging has an especially large impact for biomedical studies where the objective is to image soft tissue like muscles [6] or soft tissue encapsulated in a bony shell [7].

Resolution is limited by the detector performance but can be drastically improved by increasing the sample's X-ray projection on the detector plane. With X-ray optics, it is possible to build optical instruments for the hard X-ray regime similar to those used for visible light. We built a hard X-ray microscope using a Kirkpatrick–Baez mirror as the condenser optics and a Fresnel–Zone plate as the high-resolution objective lens. The instrument can image 50-nm structures and is ideal for high-resolution and non-destructive imaging.

doi:10.1049/mnl:20065060

Paper first received 28th September 2006 and in revised form 3rd February 2007

C. Rau, V. Crecea, K.M. Peterson, P.R. Jemian, X. Yu, P.V. Braun and T.-C. Chiang are with the Frederick-Seitz Materials Research Laboratory, University of Illinois at Urbana-Champaign, 104 South Goodwin Ave., Urbana, IL 61801, USA

C. Rau is also with the Advanced Photon Source, Argonne National Laboratory, 9700 S. Cass Ave., Argonne, IL 60439, USA; Purdue University, 480 Stadium Mall Dr., West Lafayette, IN 47907-2050, USA and National Institute of Standards and Technology, 100 Bureau Drive, Gaithersburg, MD 20899, USA

V. Crecea and T.-C. Chiang are also with the Department of Physics, University of Illinois at Urbana-Champaign, 1110 West Green, Urbana, IL 61801-3080, USA

C.-P. Richter is with the Department of Otolaryngology Head- and Neck Surgery, Northwestern University Feinberg School of Medicine, 303 E. Chicago Ave, Chicago, IL 60611, USA

U. Neuhäusler is with the Fakultät für Physik, Universität Bielefeld, Postfach 10 01 31, Bielefeld 33501, Germany

G. Schneider is with the BESSY GmbH, Albert-Einstein-Str.15, Berlin 12489, Germany

I. K. Robinson is with the Department of Physics and Astronomy, University College London, Gower Street, London WC1E 6BT, UK

E-mail: rau@anl.gov

In this paper, we provide an overview of the experimental possibilities with in-line phase contrast and hard X-ray microscopy.

2 Experimental

The instrument has been installed on the undulator beamline 34 ID at the Advanced Photon Source (APS), a third generation synchrotron at Argonne National Laboratory (Fig. 1). X-rays are generated in an electron storage ring by insertion devices (ID), deviating the electron path with alternating high magnetic fields. The undulator is one type of insertion device, producing a series of narrow peaks in the energy spectrum. The source size is 600 μm by 25 μm (horizontal × vertical) and the beam divergence is 30 μrad by 7 μrad (horizontal × vertical). The beam is shared between two stations. When the settings of the undulator are controlled by the 34 ID-E station, this operation mode is called 'parasitic mode'. A silicon mirror with differently coated stripes deflects the beam to the C-hutch [8]. Coating and deflection angle define the cut-off energy. At a deflection angle of 5 mrad and choosing the platinum coating, radiation above 15 keV is rejected. The fixed-exit double crystal monochromator is water-cooled and yields an energy bandwidth of $\Delta E/E = 10^{-4}$ using silicon (1 1 1) crystals over an energy range of 6–30 keV. Without using the monochromator, a single undulator harmonic can be filtered by the reflecting mirror, together with air absorption or an absorption filter acting as a band-pass filter (Fig. 1*a*, left side). In this case, the photon flux is 50–100 times more intense.

The experimental table is 55 m from the source. At this distance, the beam size is $\simeq 1\ \mathrm{mm}^2$. The intensity of the monochromatic beam is 10^{12} photons/s. Because of small source size s and large distance d, the transverse coherence of the beam l_{lat} is very high for a given wavelength λ: $l_{\mathrm{lat}} = d \cdot \lambda / s$. The theoretical value is 240 μm vertically by 10 μm horizontally. The longitudinal coherence length l_{lon} is given by the monochromaticity of the X-rays $\lambda/\Delta\lambda$ and the wavelength: $l_{\mathrm{lon}} = \lambda^2/\Delta\lambda$. For the monochromatic beam ($\lambda/\Delta\lambda \simeq 10^{-4}$), this value is 1.4 μm for 9-keV photon energy.

For in-line phase contrast imaging [9, 10], a sample stage and a detector are mounted on the experimental table. The distance between the sample and the detector is adjustable to modulate the contrast. The sample stage consists of several high quality translation and rotation stages, adapted to the requirements for nano-tomography. The detector registers the radiation transmitted through the sample. X-rays are transformed into visible light by a scintillation screen and then recorded via microscope optic on the chip of a CCD camera. The camera has 14-bit resolution with a 1560 × 1024 pixel array and the pixel dimension is $9 \times 9\ \mu\mathrm{m}^2$. The scintillation screen is an europium (Eu) doped Yttrium–Aluminium–Garnet (YAG) crystal. The resolution and light conversion efficiency of the crystal depend on the thickness of the doped active layer. The depth of focus and the magnification of the optical microscope are selected accordingly to the active layer thickness of the scintillation screen and the achievable resolution. For example, the resolution of the system is $\simeq 1.2$ μm when using a screen with a 6 μm thick doped active europium layer and 50× optical magnification.

The hard X-ray microscope can be set up on the same experimental table. High spatial resolution up to 50 nm is achieved with magnifying X-ray optics, such as X-ray lenses. The function of this microscope is similar to a visible light microscope. For this reason, concepts known from visible light microscopy (components, sample illumination, contrast mechanism) can be applied to the novel instrument.

For X-ray microscopy, a condenser is placed in front of the sample stage. It consists of a Kirkpatrick–Baez (KB)-mirror, which is a pair of a horizontal and a vertical platinum-coated silicon mirrors [11] (for more recent developments see [12–14]). The mirrors focus the beam in both directions onto the centre of the sample stage. The beam spot is $\simeq 3 \times 2\ \mu\mathrm{m}^2$. In order to increase the (illuminated) field of view, the condenser is scanned. The KB system is achromatic and is very light efficient and can focus more than 60% of the incoming intensity. A high resolution objective lens [15] is positioned $\simeq$2–3 mm behind the sample. Most of the beam passes straight through the zone plate without being diffracted (0th order) and does not produce a magnified image. The central part of the beam (which is close to the optical axes) is blocked by a beam-stop placed directly in front of the KB mirror system. The first diffraction order of the zone plate forms a real image in the shadow of the beam-stop.

The diameter of the zone plates is between 50 and 80 μm and their focal distance is 22.5 mm at 9-keV photon energy. The illumination by the condenser system is matched to the numerical aperture of the zone plate. Under these conditions, the full resolution of the zone plate is achieved. The outermost zone width of the zone plate Δr_{n} is 40–70 nm, providing a resolution δ between 50 and 80 nm ($\delta = 1.22 \cdot \Delta r_{\mathrm{n}}$). The zone plate has to be refocused for individual photon energies because of its chromatic aberration. In the working energy range of the microscope between 6 and 12 keV the depth of focus d_{DOF} is 15–30 μm (50-nm resolution) and 50–100 μm (85-nm resolution) given by $d_{\mathrm{DOF}} = 2 \cdot \Delta r_{\mathrm{n}}^2/\lambda$. The efficiency of the 500-nm thick gold-made zone plate is $\simeq$5% at 9-keV photon energy. With a distance of 50–70 cm between zone plate and detector, the typical X-ray magnification is between 20 and 40 times. With high X-ray magnification, a highly efficient detector configuration with moderate spatial resolution can be chosen without compromising the overall resolution of the system. Scintillation screens, such as caesium-iodide (CsI) or Eu:YAG, with 26-μm active europium layer were used for tomography experiments, providing slightly lower resolution. In this case, the exposure time is reduced from several minutes to some seconds. Complete scans with up to 180

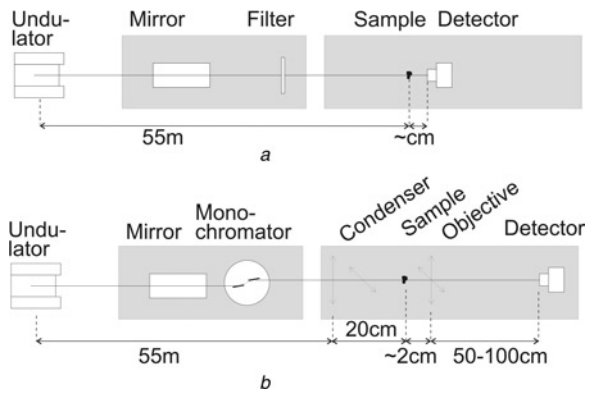

Fig. 1 *Scheme of the beamline and experiment for*

a In-line phase contrast imaging with micrometer resolution with 'Pink-beam'

b Hard X-ray microscopy on the nano-length-scale with monochromatic beam.

The condenser system in *b* consists of a horizontal and vertical focusing mirror; the focal distance for the latter is 10 cm (not represented)

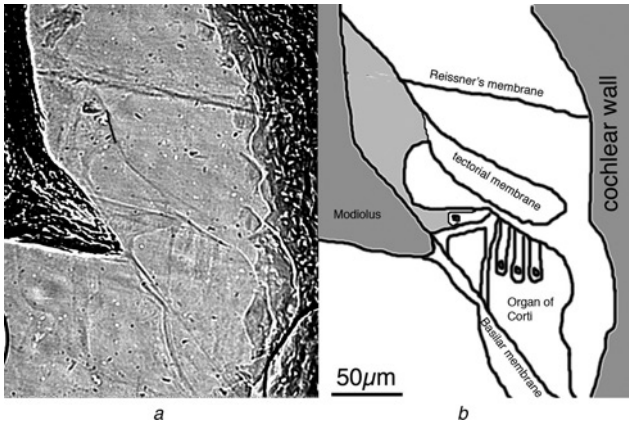

Fig. 2 *Example for the potential application of in-line phase contrast imaging*

a The sample is a thick (>300 μm) slice of a gerbil cochlea
b Fine structures of the soft tissue, such as tectorial membrane, organ of Corti, basilar membrane and Reissner's membrane, can be identified (compare with *b*)

projections were recorded within hours and less (currently under evaluation).

In-line phase contrast imaging has been used to study a mammalian cochlea and a photonic crystal. The detailed structure of photonic crystals is imaged with nanometre resolution using the hard X-ray microscope. The experimental results are presented to demonstrate the capabilities of these imaging techniques.

3 Results

Fig. 2 shows a typical result of in-line phase contrast imaging for a bio-medical application. The object is a mammalian cochlea. The photon energy was 12 keV, using monochromatic beam. For the detector a YAG crystal with a 26-μm doped Europium layer and 10× light optical magnification were chosen. Under these conditions, the spatial resolution is ≃4 μm and the exposure time 1 s. The distance between sample and detector was 20 mm. Fig. 2*a* shows the X-ray image of a thick (>400 μm) cochlea. Fig. 2*b* shows the scheme of the corresponding structures. Between strongly absorbing bone, the fine little absorbing membranes are visible. The edges are revealed by the in-line phase contrast. Structures such as the tectorial membrane, organ of Corti, basilar membrane and Reissner's membrane can be identified. This study is of major importance for further investigations with tomography or time resolved experiments. They are of particular interest to get a better understanding of the mechanism underlying the hearing process.

An application of in-line phase contrast imaging for material sciences is shown in Fig. 3. The sample is a metallic photonic crystal. It consists of an inverted nickel structure containing hollow spherical cavities. Regions of hexagonal closed packed (hcp) spheres can be identified over a large field of view. The sample thickness varies by some layers over the area. Also some disordered regions can be found (see lower right part). A part of the image is shown in detail on the lower left. The nickel walls, which separate the hollow spheres, are likely <100-nm thick. They are imaged at a detector–sample distance of 4 mm. The image was captured with a photon energy of 11 keV (monochromatic beam), an exposure time of 5 s and a detector resolution of 1.2 μm (50× optical magnification,

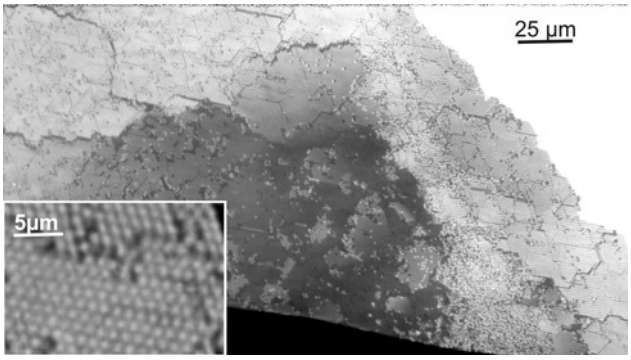

Fig. 3 *In-line phase contrast image of a photonic crystal*

The structure consists of hollow spheres in a Nickel matrix. Regions of hcp-spheres can be identified over a large field of view; the detector-sample distance was 4 mm, photon energy 9 keV, exposure time 2 s and the detector resolution 1.2 μm (Lower left: detail of the structure)

Eu:YAG screen with 6-μm thick doped active Europium layer).

Fig. 4 demonstrates the performance of the hard X-ray microscope. The X-ray magnification is 26x and the magnification of the light microscope is 50x. The pixel of the CCD chip are binned by 2 × 2. Using a 6-μm thick doped Eu:LAG screen, the exposure time is 30 s for a 13 × 5-μm^2 field of view. Again, a photonic crystal made of nickel with hollow spheres was studied (Fig. 4*a*). Details of 50-nm ligaments connecting larger structures can be identified. A profile through such a wall is shown in Fig. 4*b*. The intensity is

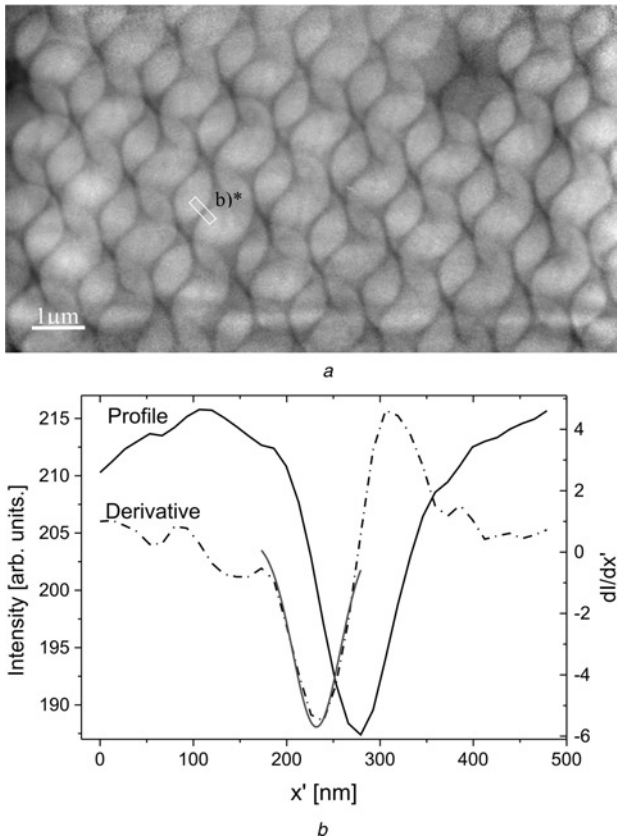

Fig. 4 *Imaging with the hard X-ray microscope*

a The sample is a photonic crystal, consisting of an inverted hollow Nickel spheres; structures as thin as 50-nm can be identified; photon energy of 9 keV was used; sample is the same as shown in Fig. 3.
b Section through ligament connecting larger structures: the dotted line represents the derivative of the profile; a Gauss curve is fit in the left part of the derivative line and its width is 50 nm (±10 nm)

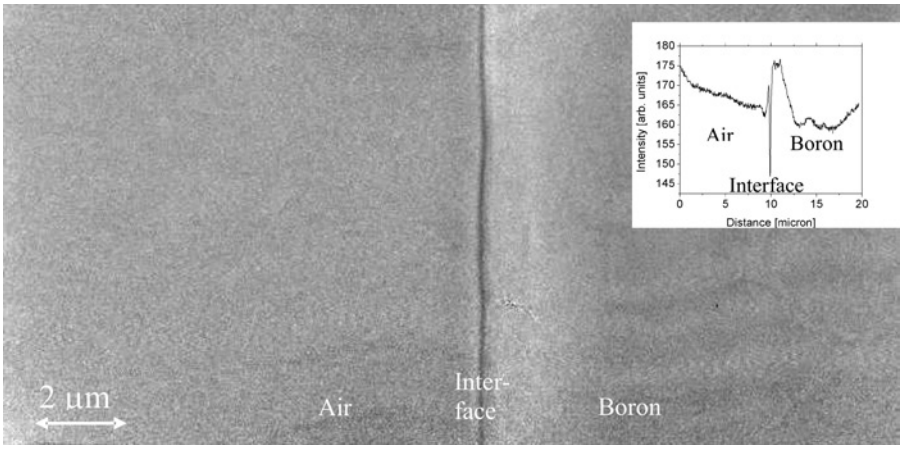

Fig. 5 *Image of a phase object with the hard X-ray microscope*

A horizontal line profile is inserted in the upper right part of the image; the sample is a boron fibre (100 µm), placed on the right side of the image and it has small absorption at the 9-keV photon energy used

A line can be identified at the interface between air and boron; the intensities on both sides of the line are very close to each other

integrated over ~140 nm perpendicular to the line. The width of the structure is ≃65 nm, measured between the inflection points of the curve. Moreover, the derivative of the profile is plotted in the same graph. The full width at half maximum (FWHM) of a Gaussian, fitted in the left branch of the curve, is 50.4 nm ± 10 nm. The latter figure is commonly used to quantify resolution, when using a knife-edge as test object. Analysing sections of broader structures give similar results to the one shown in Fig. 4*b*.

In order to prove that phase objects can be studied with the X-ray microscope, a boron fibre (with a different core) was studied as a test object (Fig. 5). The sample is nearly in focus. In the centre of Fig. 5, a fine line, corresponding to the boron–air interface can be identified. The intensities left and right of this line are almost identical as the absorption of the fibre is negligible.

4 Discussion and outlook

Synchrotron-based hard X-ray imaging is a valuable tool for micro- and nano-structured materials. Although methods like electron microscopy or atomic force microscopy have much higher spatial resolution, X-ray microscopy has an ultimate advantage for investigations on bulk samples. Tomographic data of materials that become translucent at high photon energies can be acquired straightforward. Sample handling is rather easy and many kinds of sample environments are feasible.

Further improvements of the instrument's performance are possible. Spatial resolution of 15 nm is possible using the third diffraction order of the Fresnel–Zone plates under matched illumination. The efficiency and resolution of optics can be improved for both the X-ray and visible light components. The acquisition time might be also reduced by at least one order of magnitude, using a broader part of the energy spectrum and for this purpose adapted X-ray optics. Moreover, increasing the image contrast is a very profitable option. It is useful to consider therefore the Rose signal-to-noise ratio $\mathrm{SNR}_{\mathrm{Rose}} = C\,\mathrm{sqrt}(A\,q_{\mathrm{b}})$, where C is the contrast, q_{b} the average number of photons per unit area and A the area (for more information see [16] and citations within). The Rose signal-to-noise ratio is a measure for image quality and should be at least 5, in order to reliably detect a uniform object within the considered area. For images with a given $\mathrm{SNR}_{\mathrm{Rose}}$, the number of photons diminishes by the square, when the contrast is increased linearly. One efficient way to increase the contrast is the Zernike method and has already been shown to work for X-ray energies up to 4 keV [17].

5 Conclusion

Hard X-ray imaging with synchrotron radiation is a valuable tool for different scientific fields, such as materials sciences or biomedicine. Bulk materials can be studied without extensive sample preparation. Structures with low absorption contrast are imaged on the micrometer scale making use of in-line phase contrast. Highest resolution is achieved when using a hard X-ray microscope. In this case, structures with 50-nm extension can be identified.

6 Acknowledgments

The authors thank the staff members of UNICAT for their support. They thank J. Tischler for discussions. B. Tieman's software for camera control has been used. The XMI group – in particular I. McNulty – at the Advanced Photon Source is acknowledged for discussions. The UNICAT facility at the Advanced Photon Source (APS) is supported by the US DOE under Award No. DEFG02-91ER45439, through the Frederick Seitz Materials Research Laboratory at the University of Illinois at Urbana-Champaign, the ORNL (US DOE contract DE-AC05-00OR22725 with UT-Battelle LLC), the NIST (US Department of Commerce) and UOP LLC. The APS is supported by the US DOE, Basic Energy Sciences, Office of Science under contract No. W-31-109-ENG-38. C.P.R is supported by a grant from the NSF (IBN-0415901) and I.K.R by the EPSRC. The work has been supported by the National Institute of Standards and Technology (NIST). Certain commercial materials and equipment are identified in this report only to adequately specify the experimental procedure. In no case does such identification imply recommendation by the National Institute of Standards and Technology, nor does it imply that the material or equipment identified is necessarily the best available for this purpose.

6 References

1 Joannopoulos, J.D., Villeneuve, P.R., and Fan, S.: 'Photonic crystals: putting a new twist on light', *Nature*, 1997, **386**, pp. 143–149

2 Dallos, P.: 'The auditory periphery: biophysics and physiology' (Academic Press, New York, 1973)

3 Robles, L., and Ruggero, M.A.: 'Mechanics of the mammalian cochlea', *Phys. Rev.*, 2001, **81**, pp. 1305–1352
4 von Békésy, G.: 'Experiments in Hearing' (McGraw-Hill Book Company, New York, 1960)
5 Vogel, U.: 'New approach for 3D imaging and geometry modeling of the human inner ear', *ORL – J. Oto-Rhino-Laryngology and its related specialities*, 1999, **61**, (5), pp. 259–267
6 Kohn, V., Rau, C., Sergienko, P.M., Snigireva, I., Snigirev, A., and Vazina, A.: 'The live lattices become visible in coherent synchrotron X-rays', *NIM A*, 2005, **543**, (1), pp. 306–311
7 Rau, C., Robinson, I.K., and Richter, C.-P.: 'Visualizing soft tissue in the mammalian cochlea with coherent hard X-rays', *Mater. Res. Tech.*, 2006, **69**, (8), pp. 660–665
8 Benson, C.A., and Robinson, I.K.: 'Beam splitting mirror for advanced photon source sector 34' in Pianetta, P. (Ed.): 'Eleventh US National Conference on Synchrotron Radiation Instrumentation', AIP Conference Series, 2000, pp. 230–233
9 Snigirev, A., Snigireva, I., Kohn, V., Kuznetzov, S., and Schelokov, I.: 'On the possibilities of X-ray phase contrast microimaging by coherent high-energy synchrotron radiation', *Rev. Sci. Instrum.*, 1995, **66**, (12), pp. 5486–5492
10 Spanne, P., Raven, C., Snigireva, I., and Snigirev, A.: 'In-line holography and phase-contrast microtomography with high energy X-rays', *Phys. Med. Biol.*, 1999, **44**, pp. 741–749
11 Eng, P.J., Newville, M., Rivers, M.L., and Sutton, S.R.: 'Dynamically Figured Kirkpatrick-Baez X-ray Micro-Focusing Optics' in McNulty, I. (Ed.): 'X-Ray microfocusing: applications and technique', *SPIE Proc.*, 1998, **3449**, pp. 145–155
12 Hignette, O., Cloetens, P., Rostaing, G., Bernard, P., and Morawe, C.: 'Efficient sub 100 nm focusing of hard X rays', *Rev. Sci. Inst.*, 2005, **76**, pp. 063710–5
13 Liu, W., Ice, G., Tischler, J., Khounsary, A., Liu, C., Assoufid, L., and Macrer, A.: 'Short focal length Kirkpatrick-Baez mirrors for a hard X-ray nanoprobe', *Rev. Sci. Inst.*, 2005, **76**, pp. 113701–6
14 Matsuyama, S., Mimura, H., Yumoto, H., Yamamura, K., Sano, Y., Endo, K., Mori, Y., Nishino, Y., Tamasaku, K., Ishikawa, T., Yabashi, M., and Yamauchi, K.: 'Diffraction-limited two-dimensional hard-X-ray focusing at the 100 nm level using a Kirkpatrick-Baez mirror arrangement', *Rev. Sci. Inst.*, 2005, **76**, pp. 083114–5
15 Panitz, M., Schneider, G., Peuker, M., Hambach, D., Kaulich, B., Oestreich, S., Susini, J., and Schmahl, G.: 'Electroplated gold zone plates as x-ray objectives for photon energies of 2–8 KeV' in Meyer-Ilse, T.W., and Attwood, D. (Eds.): 'Sixth International Conference X-Ray Microscopy' (American Institute of Physics, 2000), pp. 676–681
16 Cunningham, I.A., and Shaw, R.: 'Signal-to-noise optimization of medical imaging systems', *J. Opt. Soc. Am. A*, 1999, **16**, (3), pp. 621–632
17 Neuhäusler, U., Schneider, G., Ludwig, W., Meyer, M.A., Zschech, E., and Hambach, D.: 'X-ray microscopy in Zernike phase contrast mode at 4 keV photon energy with 60 nm spatial resolution', *J. Phys. D*, 2003, **36**, (10A), A79–A82